FIELD INTERCOMPARISON AND LABORATORY TESTS OF PRECIPITATION DETECTORS

Simone Griesel, Manfred Theel, Karsten Schubotz, and Eckhard Lanzinger

Deutscher Wetterdienst DWD, Frahmredder 95, 20393 Hamburg, Germany

Tel.: +49 69 8062 6522, Fax: +49 698062 6507, Email: simone.griesel@dwd.de

ABSTRACT

To determine the beginning and the end of precipitation events, currently conductive and optical detectors are used in the national meteorological network of Deutscher Wetterdienst (DWD). In a market examination seven commercially available precipitation detectors with differing measuring principles were compared:

- capacitive sensors: MPS RQA, Campbell RD01, and Vaisala DRD11
- conductive sensors: Eigenbrodt RS85 and Kroneis Precipitation Detector
- optical sensors: Thies Precipitation Monitor and RLS Wacon IRSS88

All sensors were installed at the DWD test fields Wasserkuppe (950 m asl) and Hamburg-Sasel (30 m asl). Automated measurements (Laser Precipitation Monitor [LPM], Thies) were selected as intercomparison reference.

Results are presented as contingency tables and thereof derived skill scores stratified by aggregate state (liquid, freezing and solid precipitation). We found some characteristic performance differences between the measuring principles of these detectors.

In addition a laboratory test methodology will be presented to verify the WMO sensitivity threshold of 0.02 mm/h. For this purpose liquid particles with diameters of about 200 µm are generated and applied to the detectors.

1. Introduction

In meteorological networks precipitation detectors are widely used in conjunction with precipitation gauges to identify true precipitation events and filter out false registrations.

In the national meteorological network of Deutscher Wetterdienst (DWD), precipitation detectors are also used to verify automatic present weather classifications. Therefore a sensitive, fast reacting and reliably detecting device is needed to determine the true duration of precipitation events.

In this study, sensors with different measuring principles were investigated in order to consider their advantages and disadvantages.

2. Instruments and References

Seven different precipitation detectors were investigated. Because commercially available instruments are applying capacitive, conductive and optical measuring principles, two detectors of each kind have been purchased in 2012. In March 2013 a Vaisala detector was added to the test, because it is widely used in meteorological services. Table 1 gives an overview of sensors, manufacturers, measuring principles and the sensing area of each detector together with the reference used in this study.

Table 1: Overview of the tested sensors their measurement principles and sensing areas and the reference instrument Thies LPM

Manufacturer	Sensor	Measuring principle	sensing area	output channel analogue	output channel binary
MPS	RQA	capacitive	38.5 cm^2	x	x
Campbell	RD01	capacitive	6.6 cm^2	x	x
Vaisala	DRD11	capacitive	7.2 cm^2	x	x
Eigenbrodt	RS85	conductive	60 cm^2		x
Kroneis	Kroneis	conductive	40 cm^2	x	x
Thies	5.4103.xx	optical	25 cm^2		x
RLS Wacon	IRSS88	optical	30 cm^2	x	x
Thies	LPM	optical	45 cm^2		

Capacitive sensors:
MPS RQA, Campbell RD01,and Vaisala DRD11

These precipitation detectors are based on measuring the capacitance of the precipitation deposited on the sensing element. The capacitance of the sensor element changes according to the accumulation of water on the sensor surface. The surface of the sensing areas of these sensors are set to an angle of about 30 ° to allow water to run off. Because the design is not omnidirectional, their orientation has to be considered when installing.

An integrated heater keeps it free of frost and condensation, and evaporates droplets to detect the end of a rain event and will also be activated at low temperatures to detect snow fall by melting it. Sensing areas range from 6.6 cm^2 (Campbell) to 38.5 cm^2 (MPS).
The Campbell and Vaisala sensors are provided with an external windshield to improve the sensitivity to light rain and protect the sensing element from damage.

Conductive sensors:
Eigenbrodt RS85 and Kroneis Precipitation Detector

Conductive precipitation detectors indicate the onset of precipitation by continuously monitoring the conductivity between two sections of a metal-plated grid. The rain water increases the conductivity of the grid and is detected by the circuitry which closes an internal relay.
The sensor grid contains heating elements which help to evaporate the remaining water once the precipitation has ended. When the water is completely evaporated, the conductivity of the grid decreases and the relay opens again.
The Kroneis is a cone-shaped sensor to allow water to drain off, omnidirectional and has a wind shield. The RS85 is pyramid-shaped and equipped with snow catchment pins.

Optical sensors:
Thies 5.4103.xxx, RLS Wacon IRSS88

In the case of optical sensors, precipitation particles fall through a light band, induced by light diodes (Thies) or a dual infrared beam (IRSS88), and lead to shadowing effects on the receiving diode. The transmitted light is pulse-modulated to filter out background light sources. The Thies instrument is equipped with a heating system to avoid ice and snow accretion on the housing surface. In addition, the surface retains a temperature of >0 °C by means of a controlled heating. For both sensors the sensitivity can be modified by selecting a minimum number of drop events per time interval. As optical detectors are principally operating lag free, a time interval length can be set to keep the relay contact closed for a certain time after the detection threshold has been reached.

Reference
In this study the Thies Laser Precipitation Monitor (LPM) was used as reference instrument on both test sites and was installed in close proximity to the precipitation detectors under test. The LPM is basically a laser disdrometer which determines the particle size and velocity spectrum of precipitation. It is very sensitive in detecting particles falling through the infrared laser beam. Additionally it classifies precipitation type, such as drizzle, rain, hail, snow, snow grains, graupel (small hail / snow pellets), and ice pellets. The disdrometer also calculates the intensity and amount (water equivalent). SYNOP codes according table 4680, and METAR codes according table 4678 are implemented. In former investigation the capabilities and limitations of this sensor were described [Bloemink and Lanzinger 2009].

For this study the LPM output was classified into liquid, solid and general precipitation.

3. Experimental Field Set Up

The comparisons of the precipitation detectors were taking place at two sites in parallel: at the manned DWD weather station Wasserkuppe, a mountain site at 950 m above sea level and at the test field Hamburg-Sasel, a lowland site at 30 m above sea level.

At Wasserkuppe and Hamburg all sensors under test were installed at 2 m above surface. The orientation is NW, such that the measurement surfaces/ volumes are perpendicular to the prevailing north westerly wind direction with the main precipitation to minimize the influence of asymmetric sensor constructions.

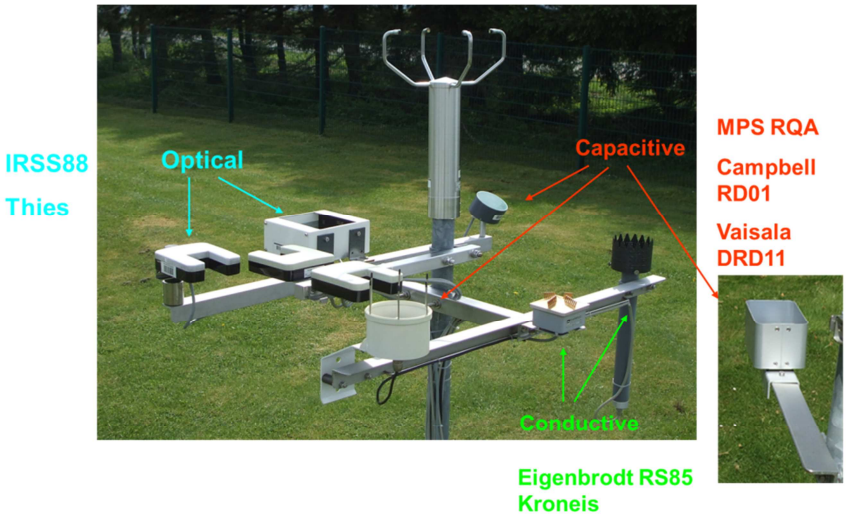

Figure 1: Field setup at Wasserkuppe, a DWD weather station at 950 m asl, under summer conditions

4. Data processing

To compare the various results of the different precipitation detectors, data were recorded at a time resolution of one minute. Results were obtained using Wasserkuppe data from 05/2012 to 05/2013 and Hamburg data from 05/2012 to 02/2013 and from 3/2013 to 5/2013 the DRD11 was added there. At Wasserkuppe the observer additionally reported the precipitation in WMO PW code 4677 for manual observations. Data from sensors with analogue output were used with different thresholds. Analogue data output signals were set to 0.1 V at Wasserkuppe and Hamburg. When installing the DRD11 at Hamburg all thresholds in Hamburg were set to 0.02 V for 1 % full scale.

Using the Thies disdrometer (LPM) as the reference allows data classification by liquid and solid precipitation. Freezing rain is classified as liquid.

Evaluation and case studies

For the first step, daily graphs were created to study the behavior of the sensors. The precipitation detections of every sensor were plotted by drawing lines from the start to the end point of the detection period (see Figure 2 and 3). The LPM is depicted in black, the observer and the optical sensors in blue, green lines are for the conductive sensors and red lines for the capacitive sensors. For some sensors (MPS, RD01 and IRSS) the analog signals were plotted as well. The little numbers above these lines represent the delay times with respect to the LPM detections.

In the separate, upper graph, the WMO PW codes 4677 recorded manually by the observer and classified to liquid, solid and freezing phases, are shown. Precipitation intensity and amount determined by the LPM is also plotted there (black and grey lines).

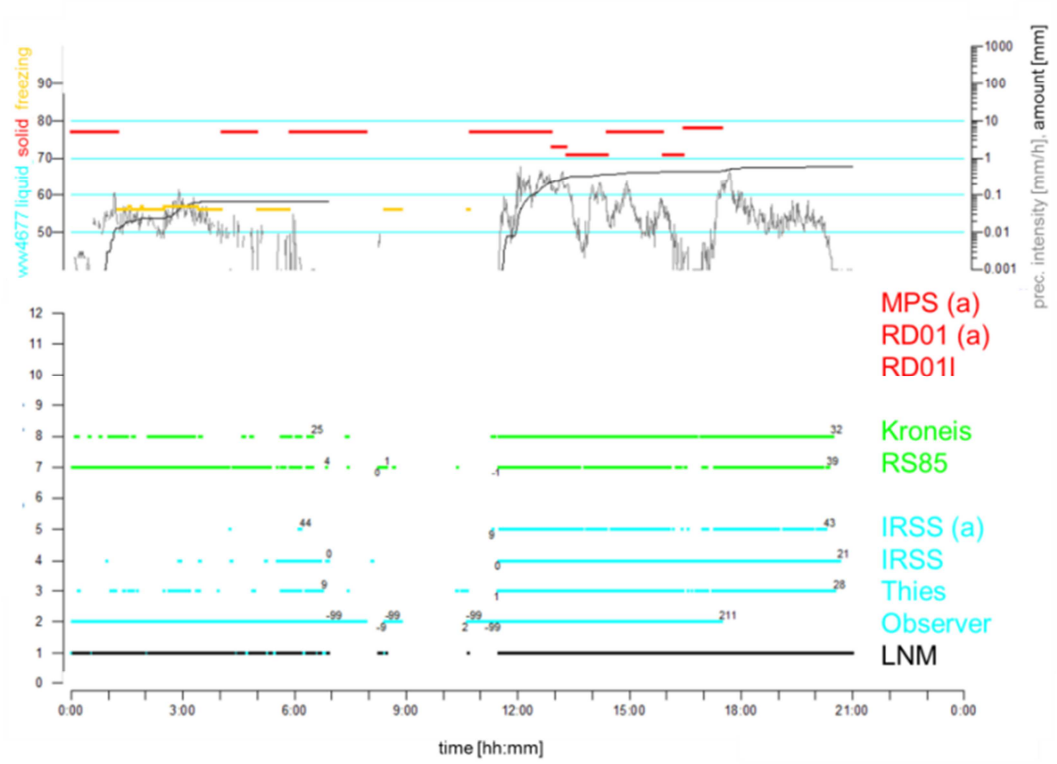

Figure 2: Example for graphic evaluation. Comparison of the precipitation detectors at Wasserkuppe. Conductive sensors do not detect the solid and freezing precipitation reported by the manual observer at the 06.04.2013.

Figure 2 reflects the situation with solid and freezing precipitation on the 06.04.2013 at the test field Wasserkuppe. All capacitive sensors (red) were not able to detect these events. The analogue output channel of the MPS an both output channels of the RD 01, the analogue and the binary, do not detect any precipitation.

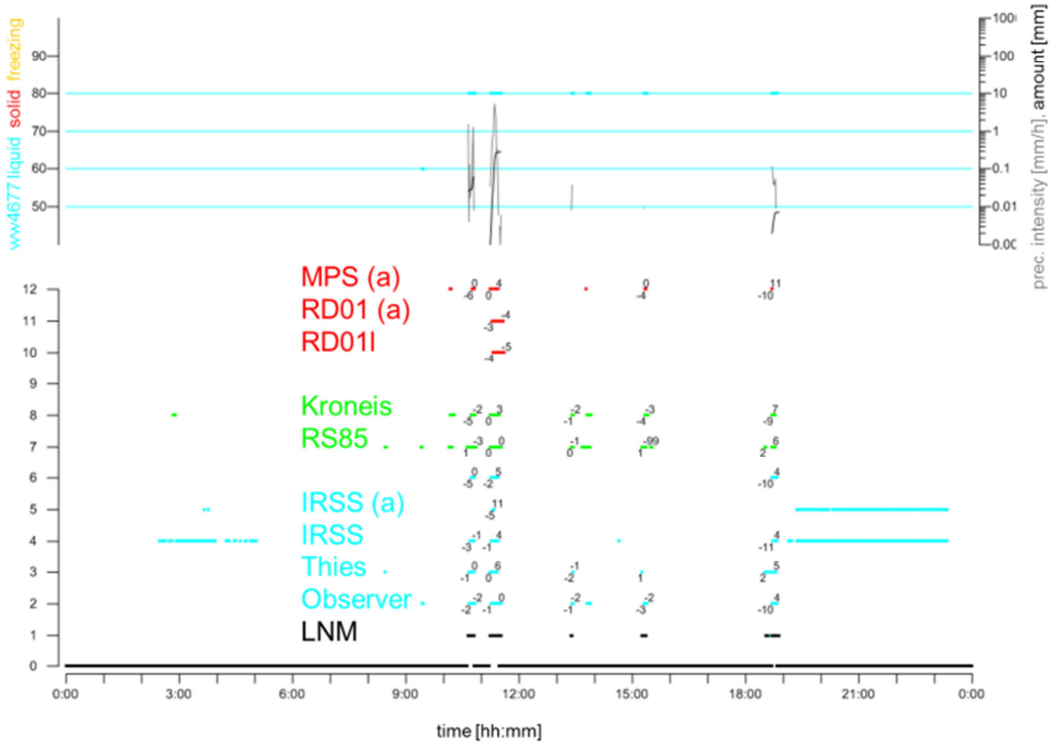

Figure 3: Comparison of precipitation detectors at Wasserkuppe [13.08.2013]. Optical sensors detect precipitation whereas the other sensors and the observer don not report any precipitation at all.

Figure 3 illustrates a weak point of optical sensors. The IRSS reports false detections due to particles in the optical path that were not caused by precipitation as can be seen in the results for all other sensors and the observer. Typically spiders and other insects are the reason for such effects.

Numerical analysis

Data of a one year field experiment (05/2012 – 05/2013) were aggregated in contingency tables and thereupon analysed by calculating skill scores with the LPM being used as relative reference.. The evaluation was run separately for liquid precipitation (together with freezing rain) and solid precipitation.
The nomenclature of the contingency table (letters a, b, c and d) was used according to [Stanski et.al. 1989]:

a- LPM and the tested sensors both report precipitation
b- LPM does not report precipitation whereas the tested sensor reports precipitation
c- LPM reports precipitation whereas the tested sensor reports no precipitation
d- LPM and the tested sensors both do not report any precipitation at all

		Reference LPM: Yes	Reference LPM: No
Tested Instrument	Yes	*hits (a)*	*false alarms (b)*
	No	*misses (c)*	*correct negatives (d)*

Probability of detection $POD = \frac{a}{(a+c)}$ with a range from 0 to 1 and perfect score of 1

False alarm rate $FAR = \frac{b}{(a+b)}$ with a range from 0 to 1 and a perfect score of 0

Frequency bias $FBI = \frac{(a+b)}{(a+c)}$ with a range from 0 to ∞ and a perfect score of 1

Heidke Skill Score $HSS = \frac{(a+d-R)}{(a+b+c+d)}$ where $R = \frac{((a+b)\times(a+c)\times(c+d)\times(b+d))}{(a+b+c+d)}$

With a range from -∞ to 1 and a perfect score of 1, 0 indicates no skill.

Results for all sensors at Wasserkuppe and Hamburg are shown in Table 2 - 4.

Table 2: Results for Wasserkuppe 05/2012 to 05/2013

ALL	Thies	IRSS	Eigenbrodt	Kroneis	Campbell (a)	MPS (a)
POD	0.83	0.79	0.73	0.78	0.27	0.28
FAR	0.09	0.17	0.13	0.08	0.03	0.01
FBI	0.90	0.96	0.84	0.86	0.28	0.28
HSS	0.83	0.75	0.73	0.80	0.36	0.37
liquid	Thies	IRSS	Eigenbrodt	Kroneis	Campbell (a)	MPS (a)
POD	0.90	0.83	0.84	0.84	0.42	0.49
FAR	0.15	0.29	0.21	0.15	0.04	0.01
FBI	1.05	1.17	1.07	0.99	0.44	0.49
HSS	0.85	0.72	0.78	0.82	0.55	0.62
solid	Thies	IRSS	Eigenbrodt	Kroneis	Campbell (a)	MPS (a)
POD	0.75	0.76	0.61	0.73	0.12	0.08
FAR	0.17	0.30	0.26	0.16	0.12	0.04
FBI	0.91	1.09	0.84	0.87	0.14	0.08
HSS	0.76	0.68	0.62	0.75	0.18	0.13

Table 3: Results for Hamburg Sasel 05/2012 to 02/2013, analogue output threshold 0.1 V

ALL	Thies	IRSS (a)	Eigenbrodt	Kroneis	Campbell (a)	MPS (a)
POD	0.86	0.28	0.81	0.85	0.42	0.37
FAR	0.06	0.01	0.09	0.10	0.06	0.01
FBI	0.91	0.28	0.89	0.94	0.44	0.37
HSS	0.88	0.38	0.83	0.85	0.53	0.49
liquid	Thies	IRSS (a)	Eigenbrodt	Kroneis	Campbell (a)	MPS (a)
POD	0.83	0.22	0.84	0.86	0.47	0.44
FAR	0.08	0.03	0.11	0.12	0.06	0.01
FBI	0.90	0.22	0.94	0.99	0.51	0.44
HSS	0.86	0.33	0.84	0.85	0.59	0.58
solid	Thies	IRSS (a)	Eigenbrodt	Kroneis	Campbell (a)	MPS (a)
POD	0.93	0.38	0.74	0.81	0.25	0.14
FAR	0.18	0.02	0.29	0.31	0.28	0.06
FBI	1.13	0.39	1.04	1.18	0.35	0.15
HSS	0.86	0.52	0.71	0.73	0.36	0.24

Table 4: Results for Hamburg-Sasel 03/2013 – 06/2013, analogue threshold 0.02 V

ALL	Thies	IRSS (a)	Eigenbrodt	Kroneis	Campbell (a)	MPS (a)	DRD11 (a)
POD	0.88	0.28	0.79	0.84	0.38	0.34	0.70
FAR	0.04	0.01	0.08	0.10	0.02	0.00	0.15
FBI	0.92	0.28	0.86	0.93	0.39	0.34	0.83
HSS	0.90	0.38	0.82	0.84	0.49	0.45	0.72
liquid	Thies	IRSS (a)	Eigenbrodt	Kroneis	Campbell (a)	MPS (a)	DRD11 (a)
POD	0.86	0.22	0.85	0.83	0.50	0.51	0.83
FAR	0.07	0.03	0.12	0.15	0.02	0.00	0.20
FBI	0.92	0.22	0.96	0.98	0.51	0.51	1.04
HSS	0.88	0.33	0.85	0.82	0.63	0.64	0.79
solid	Thies	IRSS (a)	Eigenbrodt	Kroneis	Campbell (a)	MPS (a)	DRD11 (a)
POD	0.93	0.38	0.69	0.84	0.19	0.08	0.50
FAR	0.10	0.02	0.20	0.22	0.09	0.03	0.40
FBI	1.03	0.39	0.87	1.08	0.21	0.08	0.83
HSS	0.91	0.52	0.72	0.79	0.29	0.13	0.51

5. Results

Comparison Wasserkuppe - Hamburg

Comparing the verification scores for liquid precipitation are the same for Wasserkuppe and Hamburg-Sasel for all sensors except the IRSS88 RLS Wacon. POD was around 80 % for Thies, Eigenbrodt and Kroneis, around 45 % for Campbell and MPS. The RLS provided far less detections in Hamburg compared to the results at Wasserkuppe. The reason is that in Hamburg the analogue output signal was used with a threshold of 0.1 V and 0.02 V later on whereas at Wasserkuppe the binary Y/N output was used. The frequency bias was > 100 % at Wasserkuppe for Thies, IRSS, and Eigenbrodt.

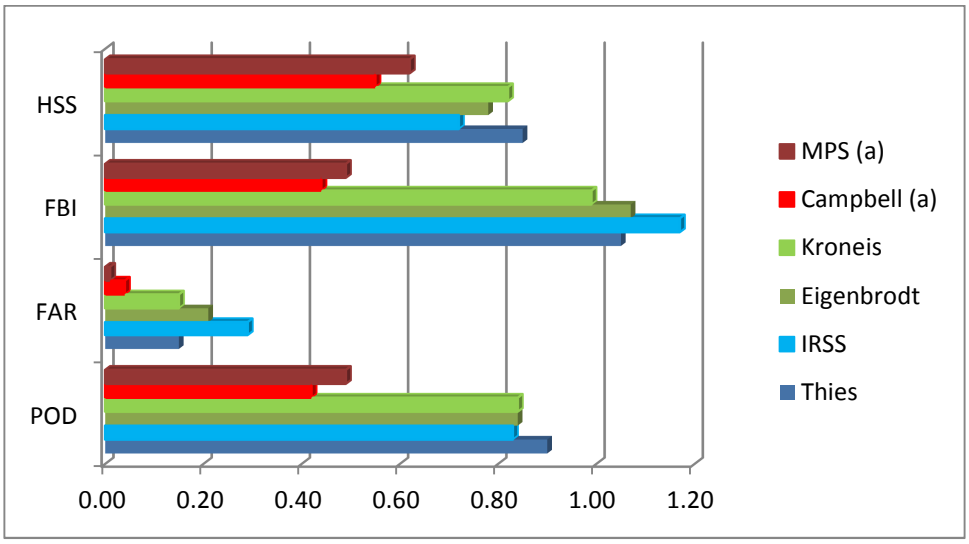

Figure 4: Results for liquid precipitation at Wasserkuppe 05/2012 to 05/2013

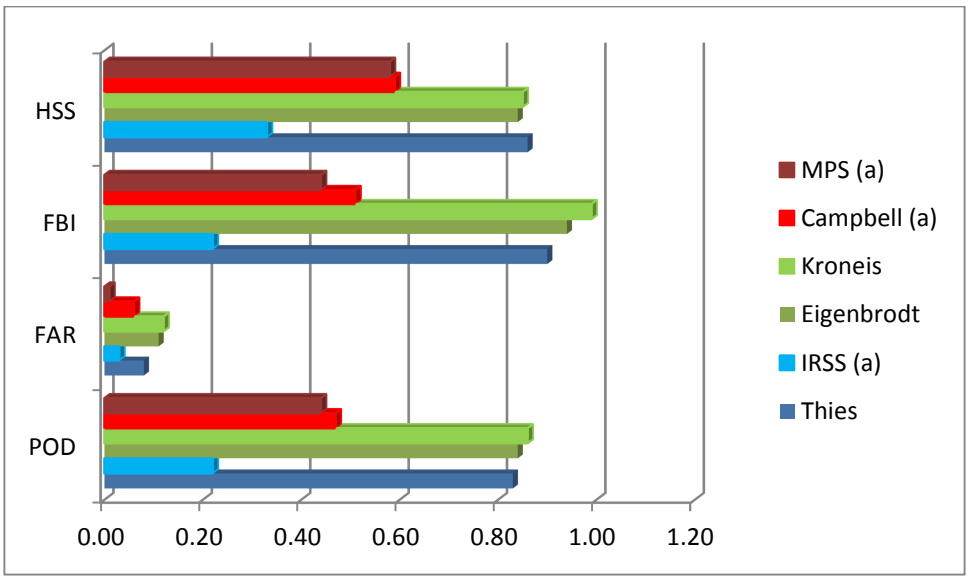

Figure 5: Results for liquid precipitation at Hamburg Sasel 05/2012 to 02/2013

The results for snow POD were higher at Hamburg but at the same time the FAR rose up to 31 % for the Kroneis and the FBI exceeded the 100% for Thies, Eigenbrodt and Kroneis.

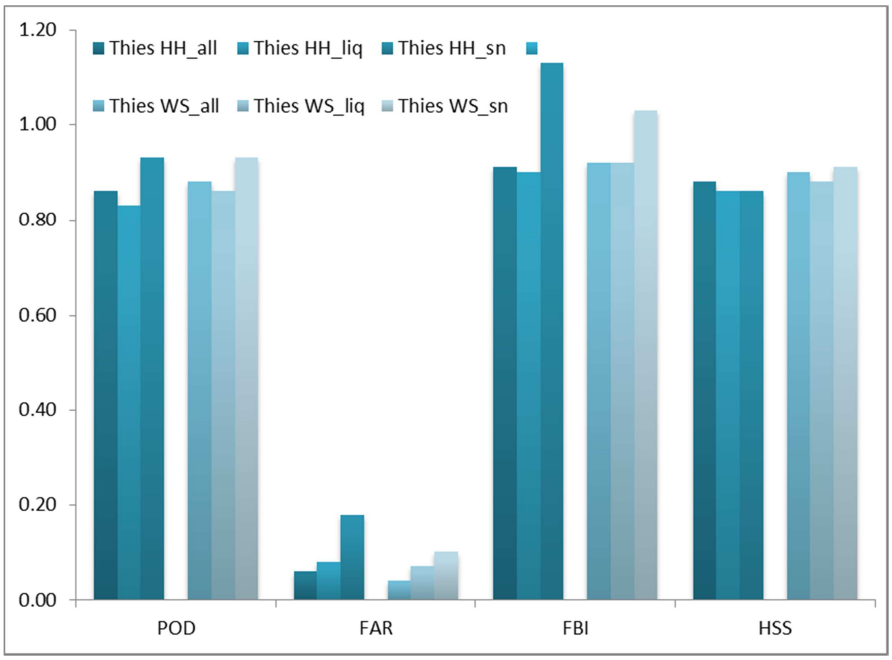

Figure 6: Results for optical precipitation detector Thies, stratified for all precipitation, liquid and solid for Hamburg (HH) and Wasserkuppe (WS).

In this study the Thies precipitation sensor showed the best results. Similar skill scores for both test sites and all kinds of precipitation could be achieved. As it is shown in Figure 6 the POD is above 80% whereas the FAR is below 10 % for liquid and 20 % for solid precipitation.

For both conductive sensors the results for POD are a little bit lower for the different kinds of precipitation at Wasserkuppe and for solid precipitation events in Hamburg but nearly the same at Hamburg for liquid precipitation. The FAR reaches 30 % for solid precipitation events in Hamburg.

Data output opportunity

Some detectors are allowing some flexibility in the selection and/or configuration of the output signal. It is quite obvious that this can be crucial for the results. All tested optical detectors (Thies, RLS IRSS) are providing a binary (Y/N) output with adjustable sensitivity and hold-on times. The IRSS is equipped with an additional analogue output. All tested conductivity detectors have a fixed binary (Y/N) output. All tested capacitance detectors are providing an analogue output signal (MPS, Vaisala, Campbell RD01) and the Campbell has an alternative binary output as well.

In this study the binary outputs were used with the settings given by the manufacturers without any modification. The Thies e.g. was set to a threshold of 2 particles per 50 s time interval and a hold-on time of 25 s. For the analogue outputs the thresholds were not optimized but rather set at a reasonable value derived by visual analysis of the data. At Wasserkuppe the threshold for MPS and Campbell was set to 0.1 V for the whole time of this study. At Hamburg the threshold for MPS, Campbell and IRSS88 was set to 0.1 V, from the 05/2012 to 02/2013. In 03/2013 the DRD11 was added and the thresholds for all sensors were reduced to 0.02 V.

As it is shown in Figure 7, results for analogue output data depend on the given threshold.

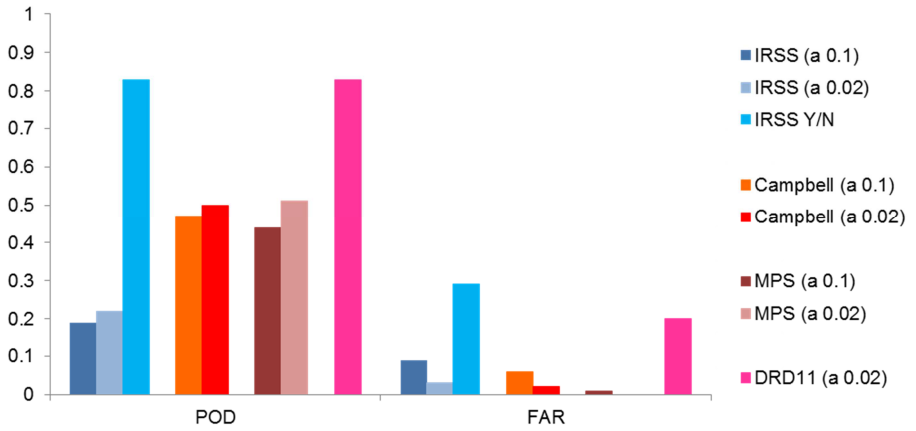

Figure 7: Skill scores (Probability of detection-POD and False alarm rate-FAR) for precipitation detectors providing different output signals. Results for liquid precipitation were plotted for binary (Y/N) and analogue output (a) with different thresholds 0.1 V and 0.02 V

By reducing the threshold from 0.1 V to 0.02 V the POD for IRSS, MPS and Campbell were increased and the FAR were reduced. The highest POD was obtained for RLS IRSS88 with binary output and the Vaisala DRD11, which in both cases is associated with an unacceptable FAR.

From this it is clear that the detection threshold of detectors with analogue output needs to be optimized for high sensitivity and low fals alarm rates.

Error sources

During freezing periods in combination with heavy snow fall the heating of most of the sensors is not sufficient to reliably melt off the snow at the detection area. In particular the sensors with wind shields accumulate snow. Figure 8 is showing this situation at Wasserkuppe.

Figure 8: Field set up at Wasserkuppe after heavy snow fall. Snow is accumulated at the wind shields of the precipitation sensors while the heating is not sufficient.

Optical sensors sometimes report false detections due to insects and spider webs etc. in the optical beam (cf. Figure 3). For asymmetric detectors the directional orientation of the sensing area can result in a significant dependency of wind direction during precipitation.

Even for the reference instrument LPM significant blocking effects due to the sensor housing were observed in a previous analysis [Lanzinger and Theel 2002]. They found average differences up to 35 % for the least ideal wind direction of differently orientated Thies LPM's.

Results of sensors with capacitive and conductive measurement surfaces can be influenced by changes of the property of the sensing surfaces due to bird droppings or a debonding of the surface layer as it is shown in Figure 9.

Figure 9: Detection areas resp. surfaces being influence by different features. 5a The MPS shows deponding of the surface layer. 5b the IRSS88 measurement were influenced by spider webs. 5c the Kroneis surface was contaminated by birds.

6. Laboratory test set up

To verify the response level of each detector for light precipitation a laboratory test methodology was developed. A *PipeJet™ nano dispenser [BioFluidiX, Freiburg, Germany]* was used to generate droplets with minimum diameters of 200 µm to reach the WMO requirements for drizzle or rain.

Presentation of a laboratory test methodology

Next to field experiments for intercomparison of rain detectors it is important to examine the performance of each sensor during a laboratory test. There are two main issues a rain detector should be checked for. The first one is the response level for low precipitation intensities. WMO defined a trigger threshold of 0.02 mm/h. The second one is the sensitivity to small droplets. According to WMO definitions, drizzle consists of liquid droplets with diameters between 200 µm and 500 µm whereas rain droplets have diameters above 500 µm. Smaller droplet diameters are found in clouds and fog.

The presented laboratory test methodology combines both requirements: a droplet dispenser drips liquid particles at a defined rate onto the detection area. The intensity of this artificial precipitation can be set by the droplet volume and rate.

The water quantity of a droplet can be calculated by the formula for a spherical volume, because photo analysis confirms this assumption. Pictures of flying droplets have been taken by a *Canon EOS 600D* dslr camera with a 1:1 macro objective and additional spacer rings. The camera was synchronized by the trigger output signal of the micro droplet dispenser. Since the camera shutter has a delay, a time delay for the release of the droplet was configured. The camera settings were:

- exposure time: 1/4000s
- focal- ratio: 5.6
- iso speed: 400

A droplet dispenser *PipeJet™ P9 nano dispenser* [BioFluidiX, Freiburg, Germany] is used in this setup. It can generate different droplet sizes at different rates. To determine the actual size of one hydrometeor, a 0.4 mm medical cannula was used as a scale in the picture [see Figure 10]. Its precise diameter of 0.406 mm had been measured by a micrometer caliper.

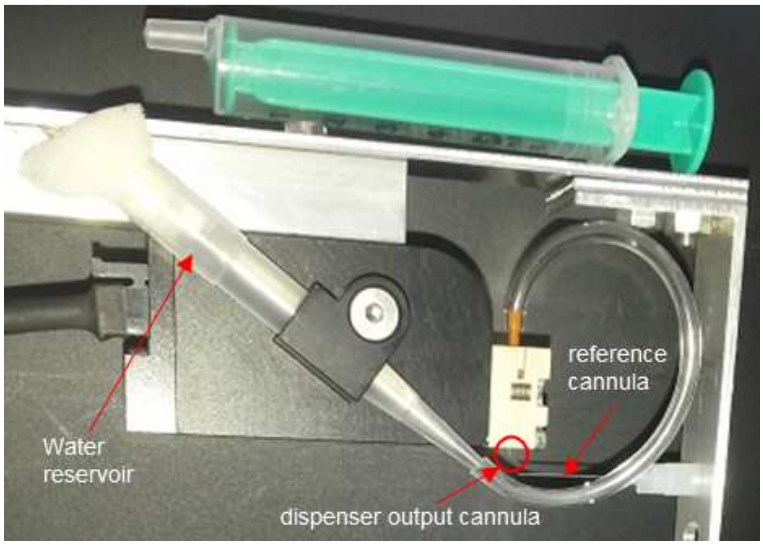

Figure 10: Laboratory set-up of the *PipeJet™ P9 nano dispenser with a medical cannula used as scale*

As an example a 0.24 mm droplet is shown in Figure 11. Changing the droplet diameter to a desired size needs some fine tuning of several dispenser parameters.

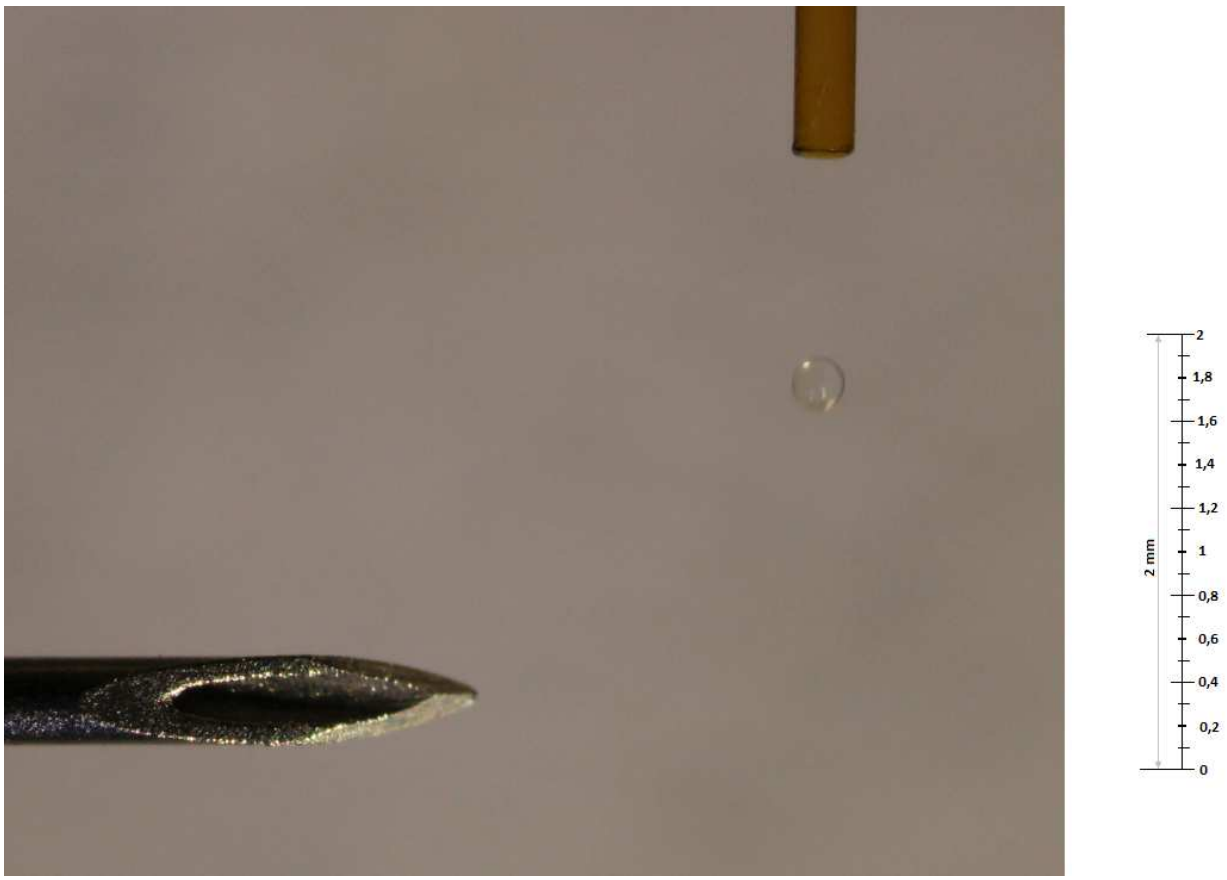

Figure 11: Droplet of 0.24 mm produced by the nano dispenser

Once the configuration is set, the droplet sizes are very uniform. The next step is to calculate the spherical volume *V* as a function of the droplet diameter *d*:

$$V(d) = \frac{4}{3} \cdot \pi \cdot \left(\frac{d}{2} \right)^3$$

As an example, the above 0.24 mm droplet has a volume of 0.0072 mm³ corresponding to 7.2 nl.

The precipitation intensity can be set by the droplet rate. It depends on the size of the measuring surface. For one square meter a particle rate of 768 drops/s of 0.24 mm diameter would be needed to reach the WMO threshold intensity of 0.02 mm/h. For a sensor surface of 50 cm^2 the droplet rate has to be 3.8 droplets per second.

To avoid an accumulation of droplets at one point on the detector and to account for differing sensitivities on the detection surface the droplets should be distributed equally over the detection surface. Therefore the droplet dispenser has to be moved over the sensor area or vice versa. We used a programmable xy- plotter for this purpose as shown in Figure 12.

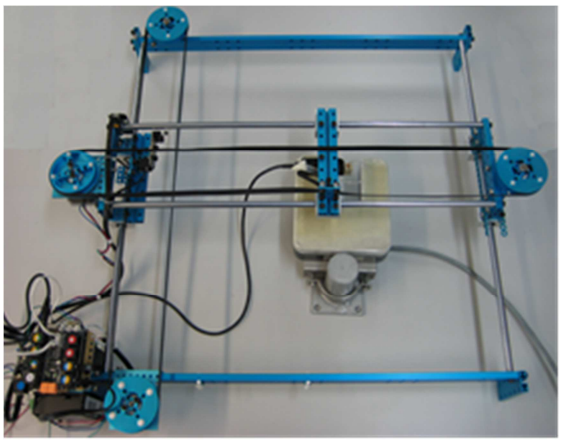

Figure 12: xy-plotter with droplet dispenser and Thies precipitation detector

7. Conclusion

In this study some experimental results are shown where several precipitation detectors have been validated in a one year comparison by Deutscher Wetterdienst (DWD).

In summary one optical detector gave the best performance followed by both conductive sensors. The capacitive sensors gave the lowest skill scores. For solid precipitation the probability of detection of the best optical detector was almost twice as much as for the best capacitive detector.

For sensors with configurable output options it is crucial to select appropriate thresholds and hold-on times for high sensitivity and low false alarm rate. Therefore analysis of further modifications for precipitation type is needed.

With the help of a laboratory methodology the WMO requirement were verified.

8. Literature

Bloemink, H.I. and Lanzinger, E. (2005): Precipitation type from the Thies didrometer. In: TECO-2005-WMO Technical Conference on Meteorological and Environmental Instruments and Methods of Observation Bucharest, Romania 4- 7 May 2005. World Meteorological Organisation, Instruments and observing methods, IOM No. 82. 3(11)

De Haijn, M. and Wauben, W. (2010): Investigation into improvement of automated precipitation type of observation at KNMI. In: TECO 2010- WMO Technical Conference on Meteorological and Environmental Instruments and Methods of Observation, Helsinki, Finland 30.8.-1.9.2010. World Meteorological Organisation, Instruments and observing methods, IOM No. 104. 3(2)

Lanzinger, E., Theel, M., Windolph, H., (2006): Rainfall amount and intensity measured by the Thies laser precipitation monitor. In: TECO-2006—WMO Technical Conference on Meteorological and Environmental Instruments and Methods of Observation Geneva, Switzerland, 4–6 December 2006. World Meteorological Organisation, Instruments and observing methods, IOM No. 94. 3(3).

Stanski, H.R., L.J. Wilson, and W.R. Burrows, (1989): *Survey of common verification methods in meteorology*. World Weather Watch Tech. Rept. No.8, WMO/TD No.358, WMO, Geneva, 114 pp.